Review

Molecular dynamics studies on 3D structures of the hydrophobic region PrP(109-136)

Jiapu Zhang[1]* and Yuanli Zhang[2]

[1]Graduate School of Sciences, Information Technology and Engineering, CIAO, The University of Ballarat, MT Helen Campus, Victoria 3353, Australia
[2]School of Basic Medical Sciences, Taishan Medical University, Tai'an 271000, China
*Correspondence address. Tel: +61-3-5327 6335; Fax: +61-3-5327 9289; E-mail: j.zhang@ballarat.edu.au

Prion diseases, traditionally referred to as transmissible spongiform encephalopathies, are invariably fatal and highly infectious neurodegenerative diseases that affect a wide variety of mammalian species, manifesting as scrapie in sheep, bovine spongiform encephalopathy (or 'mad-cow' disease) in cattle, and Creutzfeldt–Jakob disease, Gerstmann–Strussler–Scheinker syndrome, fatal familial insomnia (FFI), and Kulu in humans, etc. These neurodegenerative diseases are caused by the conversion from a soluble normal cellular prion protein (PrP^C) into insoluble abnormally folded infectious prions (PrP^{Sc}). The hydrophobic region PrP(109-136) controls the formation of diseased prions: the normal PrP(113-120) AGAAAAGA palindrome is an inhibitor/blocker of prion diseases and the highly conserved glycine-xxx-glycine motif PrP(119-131) can inhibit the formation of infectious prion proteins in cells. This article gives detailed reviews on the PrP(109-136) region and presents the studies of its three-dimensional structures and structural dynamics.

Keywords hydrophobic region; PrP(109-136); AGAA AAGA palindrome; glycine-xxx-glycine motif; molecular dynamics study

Introduction

Prion diseases such as Creutzfeldt–Jakob disease (CJD) in humans and bovine spongiform encephalopathy ('mad-cow' disease) in cattle are invariably fatal neurodegenerative diseases. Prions differ from conventional infectious agents in being highly resistant to treatments that destroy the nucleic acids found in bacteria and viruses. The infectious prion is thought to be an abnormally folded isoform (PrP^{Sc}) of a host protein known as the prion protein (PrP^C). The conversion of PrP^C to PrP^{Sc} occurs post-translationally and involves conformational change

from a predominantly α-helical protein to one rich in β-sheet amyloid fibrils. Much remains to be understood about how the normal cellular isoform of the prion protein PrP^C undergoes structural changes to become the disease-associated amyloid fibril form PrP^{Sc}. The hydrophobic domain of PrP^C(109-136) is highly conserved, containing a palindrome and the repeats of the GXXXG protein–protein interaction motif (two glycines separated by any three residues; please note that the minimum number of residues to form fibrils should be 5 [1]). It is reported that the palindrome AGAAAAGA is an inhibitor/blocker of prion diseases [1,2] and the glycine-XXX-glycine motif GAVVGGLGGYMLG is also an inhibitor of prion diseases [3–5]. The alterations of residues in AGAAAAGA and GAVVGGLGGYMLG will drastically affect the ability of cells and lead to the amyloid fibril formations (e.g. A117V will cause the Gerstmann–Straussler–Scheinker prion disease, and the numerous mutants in [3]). Our computational results also confirm the amyloid fibril formation ability of the PrP(109-136) hydrophobic region (**Fig. 1**). As shown in **Fig. 1**, if energy is less than the threshold energy −26 kcal/mol then amyloid fibril is formed in the corresponding region of residues, thus, the palindrome segment PrP(113-120) and the GLGGY segment PrP(124-128) can be firmly confirmed to have a strong amyloid fibril formation property. This paper will give detailed reviews on the PrP(109-136) region from the three-dimensional (3D) molecular structure (**Fig. 2**) point of view and presents the studies of its molecular structural dynamics. The rest of this paper is arranged as follows. Firstly, we will give a survey of the research work on AGAAAAGA and present the 3D structure of amyloid fibrils in the AGAAAAGA segment. Then, the analysis of the glycine-XXX-glycine motif GAVVGGLGGYMLG inhibiting prion diseases will be done from the molecular structural point of view. Finally, it will make some concluding remarks on the hydrophobic PrP(109-136) region.

Studies on the PrP(113-120) AGAAAAGA

A survey of the research work on AGAAAAGA

The highly conserved hydrophobic palindrome AGAA AAGA PrP(113-120) has been considered essential to PrP conformational conversion. First, we did a survey of the research work on prion AGAAAAGA listed in the PubMed database (www.ncbi.nlm.nih.gov/pubmed).

The C-terminally truncated human prion protein variant Y145Stop [i.e. HuPrP(23-144)] is a valuable model for

Figure 1 Identifying the amyloid fibril formation property   PrP(109-136) region is identified by the fibril prediction program [6] to own the amyloid fibril formation property.

understanding the fundamental properties of amyloid formation. To examine the role of AGAAAAGA segment in fibrillization of PrP(23-144), a deletion variant Δ(113-120) PrP(23-144) (in which the palindrome sequence is missing) was used [7]. The deletion results in an altered amyloid β-core without affecting amyloidogenicity or seeding specificity; this concludes that the core of some amyloids contains 'essential' (nucleation-determining) and 'nonessential' regions, with the latter being flexible in amino acid sequence space [7].

The amyloid fibrils formed by the polypeptides of PrP(113-127), AGAAAAGAVVGGLGG, are taken as the model compound to investigate the biophysical principles governing the steric zipper amyloid fibril formation [4,5,8,9]. The target fibrils adopt the structural motif of Class 7 steric zipper, which is formed by stacking of antiparallel β-sheet layers with residue 117+k forming backbone hydrogen bonds to residue 120-k [4,5,8].

Computer simulations of amyloid fibril formation by the Syrian hamster prion protein (SHaPrP) residues AGAAAA GA, the mouse prion protein (MoPrP) residues VAGAAAA GAV, and their variations GA$_6$G (a longer uninterrupted alanine stretch flanked by glycine) (AG)$_4$ (a complete disruption of hydrophobic residues), A$_8$, GAAAGAAA [a mimic of Aβ(29-36)], A$_{10}$, V$_{10}$, GAVAAAAVAG (uninterrupted hydrophobic sequence), VAVAAAAVAV [less flexible than MoPrP(111-120)] are studied previously [10]. The first two peptides are thought to act as the velcro that holds the parent
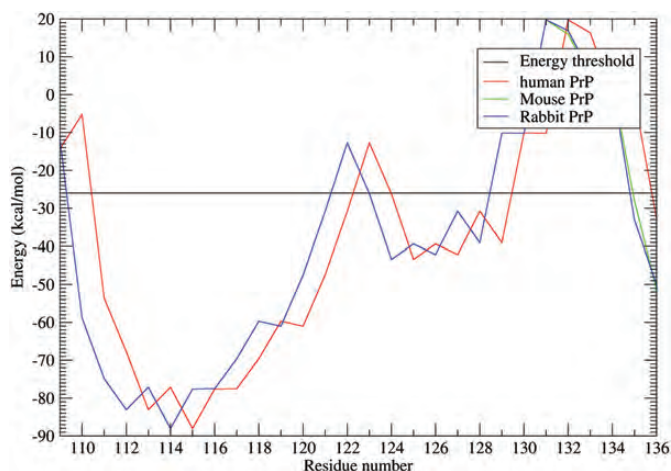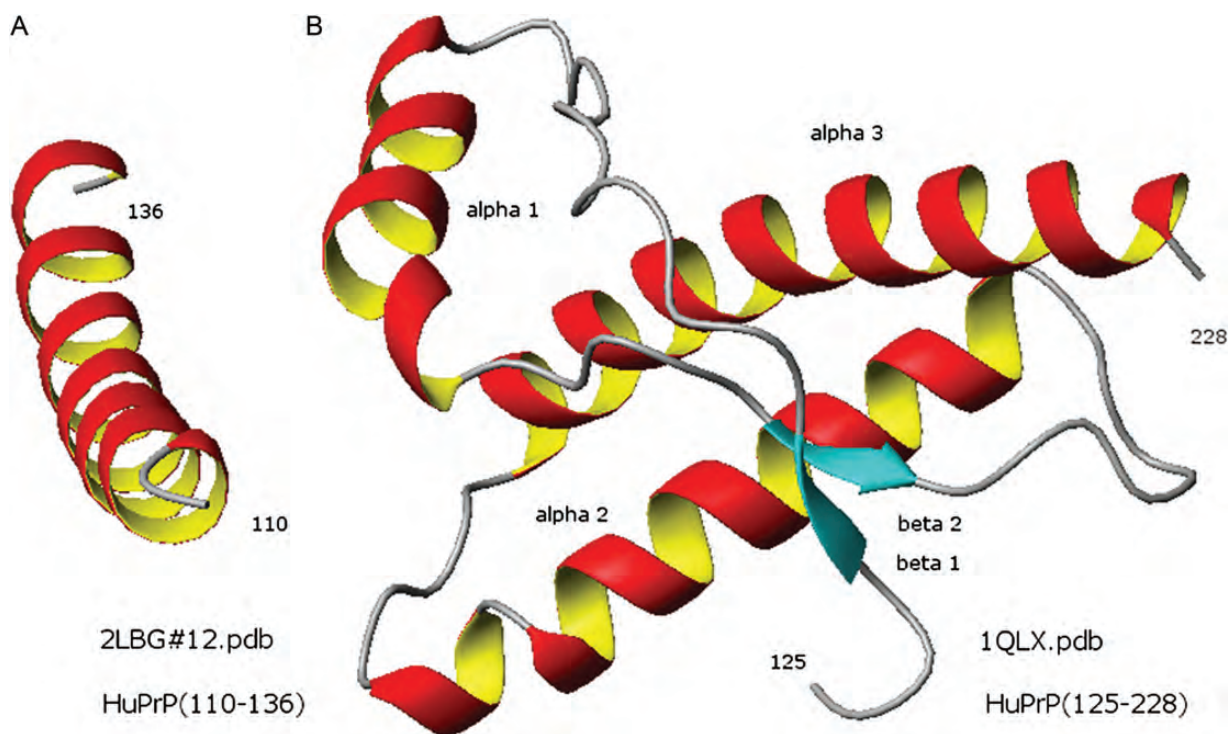

Figure 2 The 3D molecular structure of human PrP   (A) The 3D molecular NMR structure of human PrP(110-136) in dodecylphosphocholine micelles. (B) The 3D molecular NMR structure of human PrP(125-228).

prion proteins together in amyloid structures and can form fibrils themselves [10].

AGAAAAGA of HuPrP(105-210) was reported to be involved into the oligomerization and engaged in intra- and/or inter-molecular interactions [11]. The SHaPrP(109-122) peptide near the AGAAAAGA region was observed to form steric zipper fibrils by the data of crystal solid-state nuclear magnetic resonance (NMR) and molecular dynamics (MD) [5].

The cellular isoform of the prion protein PrP^C is located at the cell membrane. Studies have shown that exposure of cells to copper (Cu) causes internalization of PrP^C *in vitro*, and deletion mutation studies have shown that the palindromic region, amino acids 113-120 with the sequence AGAAAAGA is essential for copper-induced internalization to occur [12]. Kourie *et al.* [13] studied the copper modulation of ion channels of PrP(106-126) mutant prion peptide fragments and found that the hydrophobic core AGAAAAGA is not a Cu^{2+}-binding site (but at Met 109 and His ll1 ion channels can be formed).

The AGAAAAGA palindrome in PrP is required not only for the attainment of the PrPSc conformation but also to generate a productive PrP^{Sc}–PrP^C complex that leads to the propagation of PrP^{Sc} [14]. In contrast to wild-type (wt) PrP, PrP lacking the palindrome [PrP Δ(112-119)] neither converted to PrP^{Sc} nor generated proteinase K-resistant PrP. We also know that synthetic peptides corresponding to the so-called 'toxic peptide' PrP(106-126) segment form fibrils in solution with β-sheet structure [14], suggesting that PrP(106-126) segment may feature in PrP^{Sc}-PrP^C associations, and larger peptides of PrP(107-142) antagonize the *in vitro* conversion of PrP^C to the protease-resistant state in a cell-free conversion model.

Zanuy *et al.* [15] and Ma and Nussinov [16] reported that, for AGAAAAGA, the antiparallel strand orientation is preferred within the sheets but the parallel orientation is preferred between sheets. AGAAAAGA is one of the most highly amyloidogenic peptides and oligomers of AGAA AAGA were found to be stable when the size is 6 to 8 (hexamer to octamer) [16]. Here the AGAAAAGA model [16] used for their MD is a homology structure.

In a subsequent study [17], the following bioinformatics on AGAAAAGA is known. AGAAAAGA displays the highest tendency to form amyloid. Peptides containing AGAAAAGA are toxic to neurons in culture, whereby the sequence AGAAAAGA was found to be necessary but not sufficient for the neurotoxic effect [1]. The synthetic peptides derived from the central part of PrP^C(106-141) have an inhibitory effect on this conversion of PrP^C to PK-resistant PrP^{Sc}. The presence of residues 119 and 120 (the two last residues within the motif AGAAAAGA) seems to be crucial for this inhibitory effect. Mutant PrP molecules carrying deletions of amino acids 108-121 or

114-121 are not convertible to PrP^{Sc}; therefore, the central hydrophobic region, spanning all or most of the sequence AGAAAAGA, plays an important role in the PrP^{Sc}–PrP^C conversion process. Wegner *et al.* [17] assessed the effect of mutations at and around the AGAAAAGA hydrophobic sequence on protease resistance and found that mutations in the central AGAAAAGA hydrophobic region lead to immediate alterations in PrP structure and processing.

The amyloidogenic and hydrophobic core AGAAAAGA has been implicated in modulation of neurotoxicity and the secondary structure of PrP(106-126) [18,19], which is dependent on the formation of aggregated fibril structures regulated by the AGAAAAGA core [18].

Brown [1] reported that AGAAAAGA blocks the toxicity of PrP(106-126), suggesting that this sequence is necessary (but insufficient) for the interaction of PrP(106-126) with neurons and targeting or use of the AGAAAAGA peptide may represent a therapeutic opportunity for controlling prion disease.

HuPrP(106-126) has been shown to be highly fibrillogenic and toxic to neurons *in vitro*. Jobling *et al.* [19] found that the AGAAAAGA PrP(113-120) hydrophobic core sequence is important for PrP(106-126) toxicity probably by influencing its assembly into a neurotoxic structure and the hydrophobic sequence may similarly affect aggregation and toxicity observed in prion diseases.

Chabry *et al.* [20] reported that peptides from the central part of the hamster PrP 106-141 (where residues in the vicinity of positions 106-141 of PrP^{Sc} and/or PrP^C are critically involved in the intermolecular interactions that lead to PrP^{Sc} formation) could completely inhibit the conversion induced by preformed PrP^{Sc} and the presence of residues 119 and 120 from the highly hydrophobic sequence AGAAAAGA [PrP(113-120)] was crucial for an efficient inhibitory effect.

Holscher *et al.* [2] reported that the presence of AGAAAAGA of mouse PrP^C plays an important role in the conversion process of PrP^C into PrP^{Sc} and that a deletion mutant lacking these codons indeed behaves as a dominant-negative mutant with respect to PrP^{Sc} accumulation.

PrP AGAAAAGA is the most highly amyloidogenic peptide and is conserved across all species [21,22]. Gasset *et al.* [21] reported there are similarities between the PrP sequence AGAAAAGA and that of silkworm fibroin, and the homology between PrP sequence AGAAAAGAVVG GLGG and that of spider fibroin. Thus, we may say that the hydrophobic region of PrP(109-136) should be a region to form β-sheets and amyloid polymers, instead of α-helices of the Garnier–Robson analysis [23].

The 3D structure of prion AGAAAAGA amyloid fibrils

In the above survey, we know that prion AGAAAAGA peptide has been reported to own an amyloid fibril property

(initially described in 1992 by Prusiner's group). However, there has not been traditional X-ray or NMR experimental structural bioinformatics for this octapeptide yet, due to the unstable, noncrystalline and insoluble nature of this region, which just falls within the N-terminal unstructured region of prion proteins. Studies on atomic-resolution structures of the AGAAAAGA peptide will prove useful in future experimental studies on this region, aspects of the structure or the dynamics of this region should play a role in the aggregation process, and knowledge of these may be useful for the goals of medicinal chemistry for controlling prion diseases. Zhang [24] successfully constructed three amyloid fibril models (denoted as Models 1–3) for the PrP(113-120) AGAAAAGA region. Using all the PDB templates of [8] (with PDB IDs: 2OKZ, 2ONW, 2OLX, 2OMQ, 2ON9, 2ONV, 2ONA, 1YJO, 2OL9, 2OMM, 2ONX, 2OMP, 1YJP), simulation conditions are completely consistent with the previous experimental work [8] and the simulation methods of package Amber 10 [25] are the optimization steepest descent (SD) method and conjugate gradient (CG) method to relax the Models, then the standard simulated annealing method to make the equilibration of Models sufficiently stable and then the SD−CG optimization methods to refine the Models. Model 1 and Models 2 and 3 belong to Class 7 and 1 in the previous work [8], respectively, i.e. Model 1 is β-strand antiparallel, face = back, up−up (**Fig. 3**) (where numerical results show the agreement with [4,16]), and Models 2 and 3 are β-strand parallel, face-to-face, up−up (**Figs. 4** and **5**). In all

these models, there is about 5 Å between the two closest adjacent β-sheets, maintained by hydrophobic bonds, and about 4.5 Å between the two closest adjacent β-strands, which are linked by hydrogen bonds (HBs). Illuminated by PDB templates 3FVA, 3NHC/D, 3NVF/G/H/E, 3MD4/5, 2OMP, computational approaches of global optimization, local search energy minimization, simulated annealing, and structural bioinformatics etc. or introducing novel mathematical formulations and physical concepts into molecular biology may allow us to obtain a description of the protein 3D structure at a submicroscopic level for prion AGAAAAGA amyloid fibrils [24,26−30].

Structural Studies on the PrP(119-131) GAVVGGLGGYMLG

Some 30 segments from the Alzheimer's amyloid-β (Aβ) and tau proteins, the PrP prion protein, insulin, etc. form amyloid-like fibrils, microcrystals that reveal steric zipper structures [8]. Harrison *et al*. [3] reported that there are similarities between Aβ and PrP in the segment of the three GxxxG repeats (where both Aβ and PrP have the crucial residue methionine located in the middle (GxMxG) of the last repeat) [31,32] that controls prion formation. For this conserved gycine-rich region, recently, Harrison *et al*. [3] used cell biological approaches of investigating numerous mutants in this region to reveal the mechanism of prion inhibition, and mutagenesis studies demonstrated that minor alterations to this highly conserved region of PrP[C]
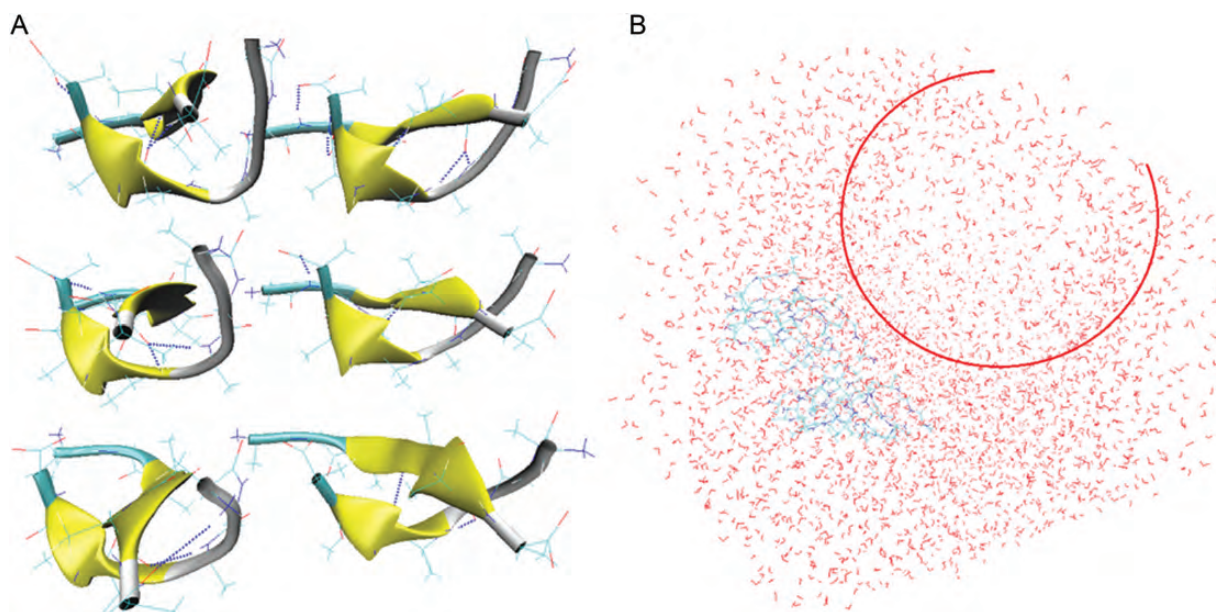

Figure 3 Model 1 for the PrP(113-120) AGAAAAGA region   (A) Blue dashed lines denote the hydrogen bonds between the pairs of β-strands, and the β-sheets are maintained by van der Waals contacts and hydrophobic packings. (B) The red circle denotes there are very few water molecules in this part of the truncated octahedral box of TIP3P waters, the trajectories of the movement of the amyloid fibril formulate a 'cage' made of waters and the amyloid fibril flies to the bottom of the 'cage', the mouth of the 'cage' is open—this illuminates to us the amyloid fibril is very hydrophobic.
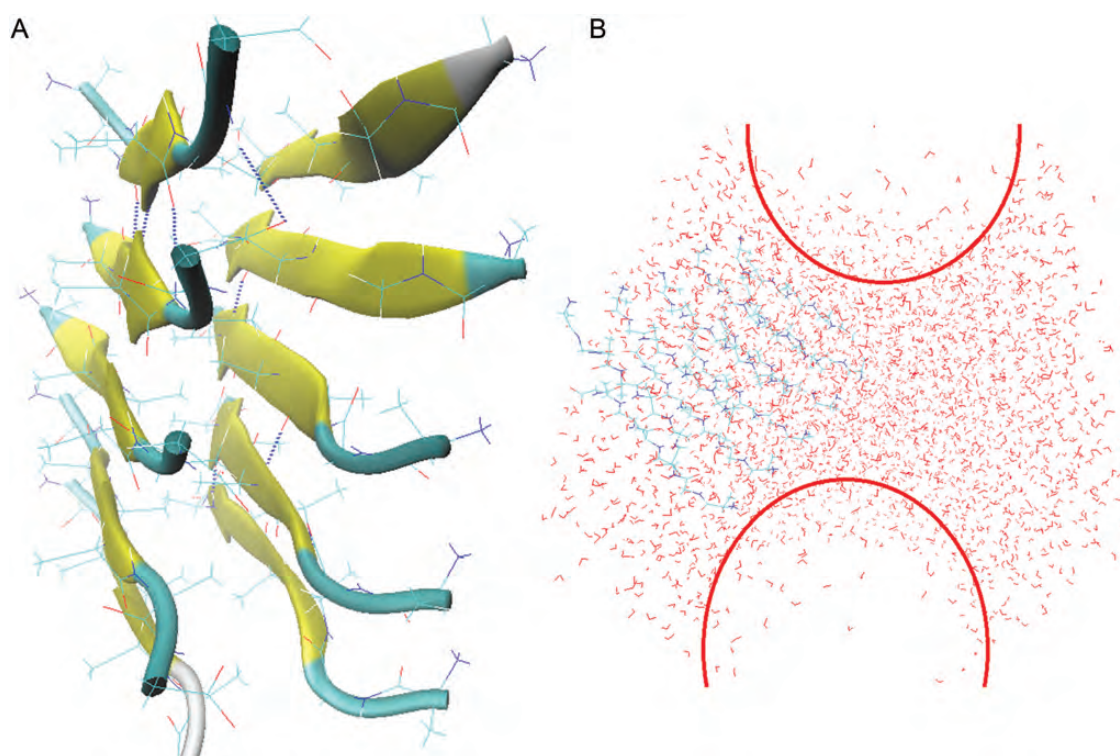
Figure 4 Model 2 for the PrP(113-120) AGAAAAGA region   (A) Blue dashed lines denote the hydrogen bonds between the pairs of β-strands, and the β-sheets are maintained by van der Waals contacts and hydrophobic packings. (B) The red half-circles denote there are very few water molecules in these parts of the truncated octahedral box of TIP3P waters, the trajectories of the movement of the amyloid fibril formulate a 'cage' made of waters with two open 'mouths' circled in red—this illuminates to us that the hydrophobic property of amyloid fibrils can form a very interesting movement pattern of trajectories.

drastically affect the ability of cells to uptake and replicate prion infection in both cell and animal bioassay. This section presents some explanations for the biological experimental performance of [3] from the molecular structural point of view.

First, we did the alignments of the structured region of mouse, human, dog, rabbit, horse, and elk PrPC (with PDB IDs 1AG2, 1QLX, 1XYK, 2FJ3, 2KU4, 1XYW, respectively) (**Fig. 6**). **Figure 6**(**A**) shows the PrP 125-136 3D structures of human, dog, rabbit, horse, and elk superposed onto mouse with backbone-atom-RMSD values 2.579427, 2.228940, 2.745877, 2.532690, 2.877734 Å respectively. In **Fig. 6**(**B**), the alignment of sequences was generated by the online CLUSTAL 2.1 program at www.ebi.ac.uk/Tools/msa/clustalw2/, where '*' means that the residues or nucleotides in that column are identical in all sequences in the alignment, ':' means that conserved substitutions have been observed, '.' means that semi-conserved substitutions are observed, the red colored residues are Small (small+hydrophobic (incl. aromatic—Y)), the blue colored residues are acidic, the green colored residues are hydroxyl + sulfhydryl + amine + G, and the gray colored residues are unusual amino/imino acids etc; the residue numbers are from 119 to 231 (for rabbit the numbers are 1 less than

others); the last column of numbers denotes the number of residues accounted from 1; the PrP 125-136 LGGYMLGSAMSR, β-strand 1, α-helix 1, β-strand 2, α-helix 2, and α-helix 3 of a PrP structure [**Fig. 2**(**B**)] were underline denoted. In **Fig. 6**, we can see that the PrP(125-136) LGGYMLGSAMSR is highly conserved among all species, strongly suggesting it has functional and evolutionary significance. To understand the functions of proteins at molecular level, in protein structures, the non-covalent interactions, such as hydrogen bonds (HBs), ionic interactions (SB), van der Waals forces (vdW), and hydrophobic packing (HP) are driving the proteins to be able to perform their biological functions (en.wikipedia.org/wiki/Protein_structure). Thus, in the subsequent studies, we will investigate the HBs, SBs, vdWs, HPs in the structures and their structural dynamics of LGGYMLGSAMSR of human and rabbit, GLGGYMLGSAMSR of mouse, VVGGLGGYMLGSAMSR of elk and dog, GSVVGGLGGYMLGSAMSR of horse (where S120 is special for horse, instead of A120) and structural connections with other residues/loops/sheets/helices in the C-terminal. Mutations will destroy these non-covalent interactions that well maintain the structure so the function of the prion protein. This will give clear explanations to the mutants in the Glycine-rich region
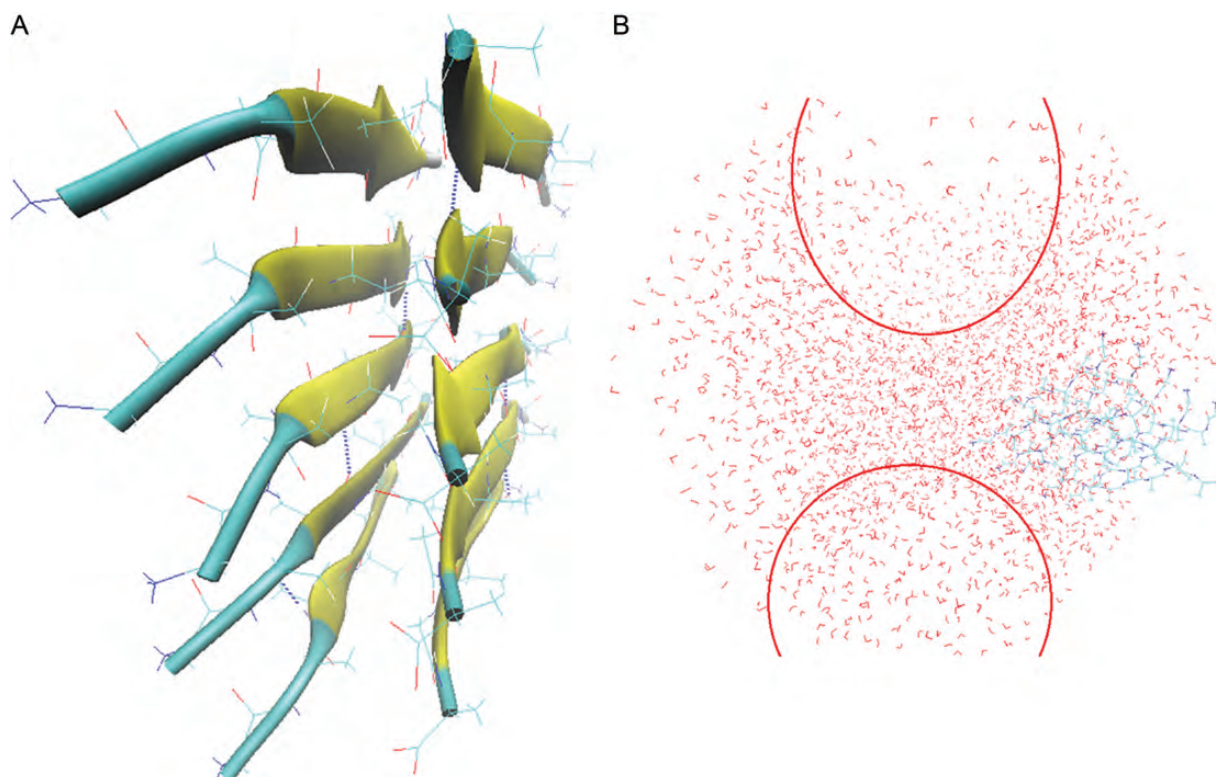
Figure 5 Model 3 for the PrP(113-120) AGAAAAGA region (A) Blue dashed lines denote the hydrogen bonds between the pairs of β-strands, and the β-sheets are maintained by van der Waals contacts and hydrophobic packings. (B) The red half-circles denote that there are very few water molecules in these parts of the truncated octahedral box of TIP3P waters, the trajectories of the movement of the amyloid fibril formulate a 'cage' made of waters with two open 'mouths' circled in red—this illuminates to us that the hydrophobic property of amyloid fibrils can form a very interesting movement pattern of trajectories, and this also illuminates us the property of periodic boundary calculations in PMEMD (Particle Mesh Eward Molecular Dynamics) simulations.
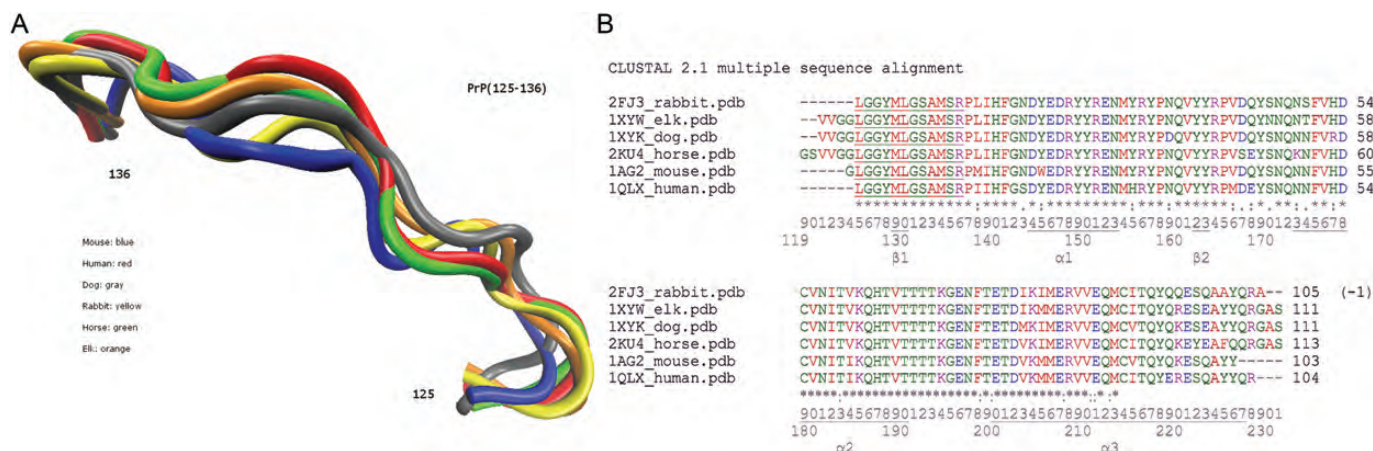

Figure 6 The alignments of the structured region of mouse, human, dog, rabbit, horse, and elk proteins with PDB IDs 1AG2, 1QLX, 1XYK, 2FJ3, 2KU4, 1XYW respectively (A) The 3D structural alignments of PrP^C(125-136), whose residues were underlined in (B). (B) The 1D sequence alignments of PrP^C(119-231).

of [3,33], which affect the uptake of prion infectivity greatly.

In 2010, horses were reported to be resistant to prion diseases [34]. First, we analyze the role of GSVVGGLG GYMLGSAMSR [PrP(119-136)] in horse PrPC(119-231)

(PDB entry 2KU4). In our study [35], the MD simulation conditions are at 350 K in explicit solvent under neutral and low pH environments, heatings are using the Langevin thermostat algorithm in constant NVT ensembles and the equilibrations and productions are using Langevin

thermostat algorithm in constant NPT ensembles. Seeing the Tables I–III of the Supplementary Material of ref. [35], we know the following HBs of GSVVGGLGGYMLG SAMSR [PrP(119-136)]:

- ARG136-TYR157 (linking β1-to-α1 loop with α1-to-β2 loop, 68.27%, 71.04%),
- MET134-ASN159 (linking β1-to-α1 loop with α1-to-β2 loop, 29.83%, 21.47%),
- GLY131-GLN160 (linking β1 with β2, 26.67%, 37.03%),
- SER132-GLN217 (linking β1 with α3, 29.70%, 12.90%),
- ARG136-PRO158 (linking β1-to-α1 loop with α1-to-β2 loop, 9.53%, 6.01%),
- ARG136-TYR157 (linking β1-to-α1 loop with α1-to-β2 loop, 68.27%, 71.04%),
- GLY126-ARG164 (linking bend before β1 with β2-to-α2 loop, 33.31%[1]),
- TYR128-ASP178 (linking coil before β1 with α2, 11.81%[1]),
- SER120-LEU125 (in the peptide, 9.72%[1]),
- LEU125-TYE128 (in the peptide, 5.58%[2]),
- GLY119-VAL122 (in the peptide, 6.51%[2]),
- GLY127-ARG164 (link bend before β1 with β2-to-α2 loop, 5.87%[2]),

where the first percentage is for seed1 (%[1]) and the second percentage is for seed2 (%[2]) and the two seeds mean two different initial velocities of 30 ns MD, and the following HPs of GSVVGGLGGYMLGSAMSR [PrP(119-136)]:

- In PrP(119-136) of 2LBG.pdb, between the two adjacent residues there are always occupied by HPs with occupied rate 100%, except for between GLY123 and GLY124, and between GLY126 and GLY127,
- Among the residues in PrP(119-136), there are HPs in
(1) TYR128-LEU130 (where LEU130 is a residue in β1),
(2) VAL121-GLY119, GLY123, TYR128, MET129, LEU130 (where MET129 and LEU130 are in β1),
(3) VAL122-SER120, GLY124, LEU125, TYR128,
(4) GLY123-SER120, LEU125,
(5) TYR128-GLY126,
(6) MET129-GLY131 (where both MET129 and GLY131 are in β1),
(7) MET134-SER132, ARG136 (where SER132 is in β1),
- The HPs between a residue in PrP(119-136) and a residue in PrP(137-231):

(1) SER135-PRO137 (where SER135, PRO137 is in β1-to-α1 loop),

(2) ARG136-MET154, TYR157 (where ARG136 is in β1-to-α1 loop, MET154 and TYR157 are in α1-to-β2 loop),
(3) ASN159-SER135, ALA133, ARG136, MET134 (where ASN159 is in α1-to-β2 loop),
(4) TYR162-TYR128, MET129, LEU130 (where MET 129, LEU130 are in β1, and TYR162 is in β2, there is no HB between TYR162 and LEU130),
(5) GLN217-GLY131 (where is in β1, GLN217 is in α3),
(6) ARG164-GLY127, MET129, TYR128 (where MET129 is in β1, ARG164 is in β2-to-α2 loop),
(7) TYR163-TYR128, LEU130, MET129 (where MET129, LEU130 are in β1, TYR163 is in β2),
(8) GLN162-ALA133, LEU130, MET134, GLY131, SER132 (where ALA133, LEU130, GLY131, SER132 are in β1, GLN162 is in β2),
(9) VAL161-GLY131, LEU130 (where GLY131, LEU 130 are in β1, VAL161 is in β2),
(10) MET213-MET134 (MET213 is in α3, MET134 is in the β1-to-α1 loop),

with >50% occupancy rate over the long MD trajectory of 30 ns. The mutations listed in Harrison's article [3] will break these HBs and HPs to lose the inhibition to prion diseases of horses.

Rabbits are also resistant to infection from prion diseases from some species [36–40] and the outbreak of 'mad rabbit disease' is unlikely [41,42]. Nisbet *et al.* [43] reported that there is 87% sequence homology between mouse PrP and rabbit PrP, approximately 9 of the 33 (i.e. 1/3) of the difference in the region DGRRSSSTV of mouse and QRAAGVL of rabbit, and residues surrounding the glycosylphosphatidylinositol anchor attachment site of PrP modulate prion infection. Under the MD simulation conditions of 450 K in explicit solvent, neutral and low pH environments, with heatings using the Langevin thermostat algorithm in constant NVT ensembles and the equilibrations and productions using Langevin thermostat algorithm in constant NPT ensembles, we have found that rabbit PrP has the C-terminal residue R227 forming a HB/SB network with inner residues and the beginning residues of rabbit homology structure PrP(120-229) (6EPA.pdb) and NMR structure PrP(124-228) (2FJ3.pdb) but mouse PrP has no such an Arginine residue at the end of C-terminal owning this property [44,45].

Dogs were reported in 2008 to be resistant to infection from prion diseases from other species [46]. In our recent work [47], MD studies were done under 450 K in explicit solvent, neutral and low pH environments, with heatings using the Langevin thermostat algorithm in constant NVT ensembles and the equilibrations and productions using Langevin thermostat algorithm in constant NPT ensembles.

In the hydrophobic region 121-136 of dog PrP, MD studies find that there are strong HBs S132-Y163-Y128 linking the two antiparallel β-strands, and strong HPs M134-A133, M129-L130, V121-V122 residing in the core of the hydrophobic region 121-136 [47]. We should note that residue 129 for dog PrP is L129 (www.uniprot.org/uniprot/O46501) but for many others is M129.

For the hydrophobic region PrP(109-136), we should also notice the following points:

- the segment GYMLGS or GYVLGS of HuPrP (127-132) can form Class 8 antiparallel amyloid fibrils (3NHC.pdb and 3NHD.pdb) [7,48],
- the mutants A117V and M129V cause GSS [49–51] and CJD [52,53] respectively,
- the β-sheet core of PrPSc consists of three layers of β-strands E1(116-119), E2(129-132), and E3(160-164) [54], where E1 and E2 are in the hydrophobic region (109-136),
- H111 is a residue of copper binding sites [55–58],
- Y128 is in the center of HB-and-SB-network of HB(Y128-D178), SB(D178-R164), HB(Y128-R164), HB(Y128-H177), HB(H177-N154) [59–62],
- A133 and S132 have HBs with R220 and a water-binding site with G131 [63,64], at S132 one O-linked sugar cannot affect the coil-to-beta structural transition of prion peptide but at S135 the effect is opposite, in PrP(113-132) the hydrophobic cluster with vdWs rendering of atoms in residues 113–127 interacts with the first β-strand (see Fig. 2(B) of [65]), M129 makes interactions with the side chain of V122 and pulls the N-terminus into the β-sheet [61] and M129 is very close to Y163 [31],
- conservation of the Gly-rich region PrP(119-131) is required for uptake of prion infectivity [3,66,67], which is shown by the physical or chemical properties of numerous mutations in the PrP(119-131) Gly-rich region [3], etc., and
- the NMR structure of HuPrP(110-136) in dodecylphosphocholine micelles was known (2LBG.pdb) [68] and we do MD simulation studies for it as follows.

We used the ff03 force field of the AMBER 11 package [69], in a neutral pH environment. The systems were surrounded with a 12-Å layer of TIP3PBOX water molecules and with 2 Cl-ions added using the XLEaP module of AMBER 11. The templates used are the 2LBG.pdb from the Protein Data Bank and its 17 mutants at G114V, A117V, G119A, G119L, G119P, A120P, G123A, G123P, G124A, L125A, G126A, G127A, G127L, M129V, G131A, G131L, G131P, which are got by the mutate module of the free package Swiss-PdbViewer version 4.1.0 (spdbv. vital-it.ch). These 18 models were firstly optimized by the

SD method and then CG method for two stages. Minimization Stage 1 is holding the solute fixed with a force constant of 500.0 kcal mol^{-1} Å^{-2} for 500 steps of SD minimization followed by 500 steps of CG minimization. Minimization Stage 2 is minimizing the entire system for 1000 steps of SD minimization followed by 1500 steps of CG minimization. The minimized models were checked by Swiss-PdbViewer and found there is not any bad contact that makes amino acids clashed. Then, the solvated proteins were quickly heated from 0 to 310 K linearly for 300 ps and then systems were kept at 310 K for 700 ps. The systems were in constant NVT ensembles using Langevin thermostat algorithm with weak restraints (a force constant of 10.0 kcal mol^{-1} Å^{-2}) on the solvated proteins. The SHAKE and PMEMD algorithms with nonbonded cutoffs of 12 angstroms were used. Next, the systems were done MD simulations in constant NPT ensembles (with constant pressure 1 atm and constant temperature 310 K) under the Langevin thermostat for 4 ns and the PRESS, VOLUME (DENSITY) and RMSD were sufficiently stable for each of the 18 models. A step size of 2 fs was used for all the MD simulations, the structures were saved to file every 1000 steps and the Metropolis criterion was used. These MD simulation conditions are completely consistent with the experimental work of NMR structure of HuPrP(110-136) (2LBG.pdb).

We picked out the snapshots at 0, 1, 2, 3, 4, and 5 ns for each model and found the α-helix structure of each model has been unfolding and longer MD simulations might make the α-helical structure unfolded completely. This shows that the PrP(110-136) region is structurally unstable and might be critical to the conversion from the predominantly α-helical PrP^C into the rich β-sheet PrP^{Sc}.

The preliminary findings to explain the above performance during the 5 ns of MD simulations may be described as follows. At the beginning of the simulations, the 3D structures of all the 13 models are α-helices. In an ideal α-helix, there are 3.6 residues per complete rotating so a rotation of 100° per residue. Thus, in all the 13 models, there are about seven turns in each α-helix. An α-helix is maintained by HBs. Clearly, the disappearance of HBs is a reason for the unfolding of all the 13 models. At the beginning of the MD simulations (i.e. at 0–1 ns), there are rich HBs in the α-helical structure of each model. But as the progress of MD simulations, most of them have disappeared, except for the three main HBs GLY/ALA/LEU/PRO131-SER135-ARG136, TYR128-SER132, which have different occupied rate for each model (**Table 1**) and are just in the N-terminal of the structural region of HuPrP(125-228) (1QLX.pdb). This might show that PrP(110-124) region of PrP(110-136) (2LBG.pdb) is very unstable. We also found that there is a SB between HIS111-LYS110 with the occupied rate 100% for the 13 models. Specially for the mutants G127L, M129V, G131A,

Table 1 Occupied rate (>10%) of the HBs for each model

	131−135	135−136	128−132	125−135	132−135	112−111
PrP(110-136)	25.48			17.68		
G114V	26.28	21.72				
A117V	40.52	8.12	8.88			
G119A	49.24	14.60	5.68			
G119L	22.80	23.96			15.08	
G119P	31.24	24.40	10.08			
A120P		35.80	5.04			
G123A	28.08	17.76	6.16			
G123P	25.52	21.92				
G124A	41.4	21.40	5.56			
L125A	36.24	17.92	5.60			
G126A	46.36	14.12	7.04			
G127A	26.20	14.88				13.08
G127L	21.20	23.60				
M129V	34.40	13.20	8.92			
G131A	47.76	13.48	17.08			
G131L	70.40	18.40	7.88			
G131P	32.48	16.72	15.20			

and G131L, there is another SB between HIS111-136ARG linking the head and the tail of HuPrP(110-136). Seeing the snapshots of 3, 4, and 5 ns of mutant G127L, 4 and 5 ns of mutant M129V, 3, 4, and 5 ns of mutant G131A, and 3, 4, and 5 ns of mutant G131L, we may know the SB HIS111-136ARG makes these snapshots looking like a 'hairpin.' The residue HIS111 is an important residue in PrP(110-136). Along with the unfolding of α-helical structure of all these 13 models, we found many HPs disappeared except for some fundamental ones MET134-ALA133, LEU130-129MET, VAL122-VAL121-ALA120, ALA118-ALA117-ALA116-ALA115, and ALA113-MET112 with the occupied rate 100%, where ALA 118-ALA117-ALA116- ALA115 are in the core of the palindrome AGAAAAGA and this might imply to us the hydrophobic core is very hard to break and this palindrome really has enormous potential to be amyloid fibrils.

Concluding Remarks on PrP(109-136)

To really reveal the secrets of prion diseases is very hard. For us it is a long shot but certainly worth pursuing. It was reported that the hydrophobic region PrP(109-136) controls the formation into diseased prions: the AGAAAAGA palindrome and glycine-xxx-glycine repeats (both being the inhibitor of prion diseases) are just in this region. This paper gives some investigations and explanations on the PrP 109-136 region in view of its 3D structures and molecular dynamics studies. The structural bioinformatics presented in this paper can be used as a reference in 3D images for laboratory experimental works. This presents some clues or hints for the study of prion proteins and prions.

Funding

References

1 Brown DR. Prion protein peptides: optimal toxicity and peptide blockade of toxicity. Mol Cell Neurosci 2000, 15: 66−78.

2 Holscher C, Delius H and Burkle A. Overexpression of nonconvertible PrP[C] delta114-121 in scrapie-infected mouse neuroblastoma cells leads to trans-dominant inhibition of wild-type PrP[Sc] accumulation. J Virol 1998, 72: 1153−1159.

3 Harrison CF, Lawson VA, Coleman BM, Kim YS, Masters CL, Cappai R and Barnham KJ, et al. Conservation of a glycine rich region in the prion protein is required for uptake of prion infectivity. J Biol Chem 2010, 285: 20213−20223.

4 Cheng HM, Tsai TWT, Huang WY, Lee HK, Lian HY, Chou FC and Mou Y, et al. Steric zipper formed by hydrophobic peptide fragment of Syrian hamster prion protein. Biochem 2011, 50: 6815−6823.

5 Lee SW, Mou Y, Lin SY, Chou FC, Tseng WH, Chen CH and Lu CY, et al. Steric zipper of the amyloid fibrils formed by residues 109-122 of the Syrian hamster prion protein. J Mol Biol 2008, 378: 1142−1154.

6 Zhang ZQ, Chen H and Lai LH. Identification of amyloid fibril-forming segments based on structure and residue-based statistical potential. Bioinformatics 2007, 23: 2218–2225.

7 Jones EM, Wu B, Surewicz K, Nadaud PS, Helmus JJ, Chen S and Jaroniec CP, et al. Structural polymorphism in amyloids: new insights from studies with Y145Stop prion protein fibrils. J Biol Chem 2011, 286: 42777–42784.

8 Sawaya MR, Sambashivan S, Nelson R, Ivanova MI, Sievers SA, Apostol MI and Thompson MJ, et al. Atomic structures of amyloid cross-beta spines reveal varied steric zippers. Nature 2007, 447: 453–457.

9 Kajava A, Squire JM and Parry DAD. Fibrous Proteins: Amyloids, Prions and Beta Proteins, Advances in Protein Chemistry. Elsevier, 2006, volume 73.

10 Wagoner VA, Cheon M, Chang I and Hall CK. Computer simulation study of amyloid fibril formation by palindromic sequences in prion peptides. Proteins 2011, 79: 2132–2145.

11 Sasaki K, Gaikwad J, Hashiguchi S, Kubota T, Sugimura K, Kremer W and Kalbitzer HR, et al. Reversible monomer-oligomer transition in human prion protein. Prion 2008, 2: 118–122.

12 Haigh CL, Edwards K and Brown DR. Copper binding is the governing determinant of prion protein turnover. Mol Cell Neurosci 2005, 30: 186–196.

13 Kourie JI, Kenna BL, Tew D, Jobling MF, Curtain CC, Masters CL and Barnham KJ, et al. Copper modulation of ion channels of PrP[106–126] mutant prion peptide fragments. J Membr Biol 2003, 193: 35–45.

14 Norstrom EM and Mastrianni JA. The AGAAAAGA palindrome in PrP is required to generate a productive PrP^{Sc}-PrP^C complex that leads to prion propagation. J Biol Chem 2005, 280: 27236–27243.

15 Zanuy D, Ma B and Nussinov R. Short peptide amyloid organization: stabilities and conformations of the islet amyloid peptide NFGAIL. Biophys J 2003, 84: 1884–1894.

16 Ma BY and Nussinov R. Molecular dynamics simulations of alanine rich β-sheet oligomers: insight into amyloid formation. Protein Sci 2002, 11: 2335–2350.

17 Wegner C, Romer A, Schmalzbauer R, Lorenz H, Windl O and Kretzschmar HA. Mutant prion protein acquires resistance to protease in mouse neuroblastoma cells. J Gen Virol 2002, 83: 1237–1245.

18 Kourie JI. Mechanisms of prion-induced modifications in membrane transport properties: implications for signal transduction and neurotoxicity. Chem Biol Interact 2001, 138: 1–26.

19 Jobling MF, Stewart LR, White AR, McLean C, Friedhuber A, Maher F and Beyreuther K, et al. The hydrophobic core sequence modulates the neurotoxic and secondary structure properties of the prion peptide 106-126. J Neurochem 1999, 73: 1557–1565.

20 Chabry J, Caughey B and Chesebro B. Specific inhibition of in vitro formation of protease-resistant prion protein by synthetic peptides. J Biol Chem 1998, 273: 13203–13207.

21 Gasset M, Baldwin MA, Lloyd DH, Gabriel JM, Holtzman DM, Cohen F and Fletterick R, et al. Predicted alpha-helical regions of the prion protein when synthesized as peptides form amyloid. Proc Natl Acad Sci USA 1992, 89: 10940–10944.

22 Govaerts C, Wille H, Prusiner SB and Cohen EE. Evidence for assembly of prions with left-handed beta-helices into trimers. Proc Natl Acad Sci USA 2004, 101: 8342–8347.

23 Garnier J, Osguthorpe DJ and Robson B. Analysis of the accuracy and implications of simple methods for predicting the secondary structure of globular proteins. J Mol Biol 1978, 120: 97–120.

24 Zhang JP. Optimal molecular structures of prion AGAAAAGA amyloid fibrils formatted by simulated annealing. J Mol Model 2011, 17: 173–179.

25 Case DA, Darden TA, Cheatham TE, III, Simmerling CL, Wang J, Duke RE and Luo R, et al. AMBER 10. San Francisco: University of California, 2008.

26 Zhang JP. Practical Global Optimization Computing Methods in Molecular Modelling − for Atomic-resolution Structures of Amyloid Fibrils. LAP LAMBERT Academic Publishing, 2011.

27 Zhang JP, Sun J and Wu CZ. Optimal atomic-resolution structures of prion AGAAAAGA amyloid fibrils. J Theor Biol 2011, 279: 17–28.

28 Zhang JP, Gao DY and Yearwood J. A novel canonical dual computational approach for prion AGAAAAGA amyloid fibril molecular modelling. J Theor Biol 2011, 284: 149–157.

29 Zhang JP. Computational potential energy minimization studies on the prion AGAAAAGA amyloid fibril molecular structures. In Bendict JB ed. Recent Advances in Crystallography. InTech Open Access Publisher, 19 Sept 2012, ISBN: 978-953-51-0754-5, Chapter 12, pp.297–312, DOI: 10.5772/47733.

30 Zhang JP, Hou YT, Wang YJ, Wang CY and Zhang XS. The LBFGS quasi-Newtonian method for molecular modelling prion AGAAAAGA amyloid fibrils. Nat Sci 2012, 4: 1097–1108.

31 Barnham KJ, Cappai R, Beyreuther K, Masters CL and Hill AF. Delineating common molecular mechanisms in Alzheimer's and prion diseases. Trends Biochem Sci 2006, 31: 465–472.

32 Harrison CF, Barnham KJ and Hill AF. Neurotoxic species in prion disease: a role for PrP isoforms?. J Neurochem 2007, 103: 1709–1720.

33 Choi JK, Park SJ, Jun YC, Oh JM, Jeong BH, Lee HP and Park SN, et al. Generation of monoclonal antibody recognized by the GxxxG motif (glycine zipper) of prion protein. Hybridoma 2006, 25: 271–277.

34 Khan MQ, Sweeting B, Mulligan VK, Arslan PE, Cashman NR, Pai EF and Chakrabartty A. Prion disease susceptibility is affected by β-structure folding propensity and local side-chain interactions in PrP. Proc Natl Acad Sci USA 2010, 107: 19808–19813.

35 Zhang JP. The structural stability of wild-type horse prion protein. J Biomol Struct Dyn 2011, 29: 369–377.

36 Vorberg I, Martin HG, Eberhard P and Suzette AP. Multiple amino acid residues within the rabbit prion protein inhibit formation of its abnormal isoform. J Virol 2003, 77: 2003–2009.

37 Lin DH and Wen Y. Progresses on prion proteins. Scientia Sinica Chimica 2011, 41: 683–698.

38 Li J, Mei FH, Xiao GF, Guo CY and Lin DH. 1H, 13C and 15N resonance assignments of rabbit prion protein 91-228. J Biol NMR 2007, 38: 181.

39 Wen Y, Li J, Xiong M, Peng Y, Yao W, Hong J and Lin DH. Solution structure and dynamics of the I214V mutant of the rabbit prion protein. PLoS One 2010, 5: e13273.

40 Wen Y, Li J, Yao W, Xiong M, Hong J, Peng Y and Xiao G, et al. Unique structural characteristics of the rabbit prion protein. J Biol Chem 2010, 285: 31682–31693.

41 Fernandez-Borges N, Chianini F, Erana H, Vidal E, Eaton SL, Pintado B and Finlayson J, et al. Naturally prion resistant mammals: a utopia?. Prion 2012, 6: 425–429.

42 Chianini F, Fernndez-Borges N, Vidal E, Gibbard L, Pintado B, de Castro J and Priola SA, et al. Rabbits are not resistant to prion infection. Proc Natl Acad Sci USA 2012, 109: 5080–5085.

43 Nisbet RM, Harrison CF, Lawson VA, Masters CL, Cappai R and Hill AF. Residues surrounding the glycosylphosphatidylinositol anchor attachment site of PrP modulate prion infection: insight from the resistance of rabbits to prion disease. J Virol 2010, 84: 6678–6686.

44 Zhang JP. Comparison studies of the structural stability of rabbit prion protein with human and mouse prion proteins. J Theor Biol 2011, 269: 88–95.

45 Zhang JP. Computational studies of the structural stability of rabbit prion protein compared with human and mouse prion proteins. In: Raymond Chuen-Chung Chang ed. Advanced Understanding of Neurodegenerative Diseases. New York: Intech Open Access Publisher, 2011, 301–310.

46 Polymenidou M, Trusheim H, Stallmach L, Moos R, Julius JA, Miele G and Lenz-Bauer C, et al. Canine MDCK cell lines are refractory toinfection with human and mouse prions. Vaccine 2008, 26: 2601–2614.

47 Zhang JP and Liu DD. Molecular dynamics studies on the structural stability of wild-type dog prion protein. J Biomol Struct Dyn 2012, 28: 861–869.

48 Apostol MI, Sawaya MR, Cascio D and Eisenberg D. Crystallographic studies of prion protein (PrP) segments suggest how structural changes encoded by polymorphism at residue 129 modulate susceptibility to human prion disease. J Biol Chem 2010, 285: 29671–29675.

49 Mastrianni JA, Curtis MT, Oberholtzer JC, Da Costa MM, DeArmond S, Prusiner SB and Garbern JY. Prion disease (PrP-A117V) presenting with ataxia instead of dementia. Neurology 1995, 45: 2042–2050.

50 Daidone I, Nola AD and Smith JC. Molecular origin of Gerstmann-Straussler-Scheinker syndrome: insight from computer simulation of an amyloidogenic prion peptide. Biophys J 2011, 100: 3000–3007.

51 Chen W, van der Kamp MW and Daggett V. Diverse effects on the native β-sheet of the human prion protein due to disease-associated mutations. Biochemistry 2010, 49: 9874–9881.

52 Klemm HM, Welton JM, Masters CL, Klug GM, Boyd A, Hill AF and Collins SJ, et al. The prion protein preference of sporadic Creutzfeldt-Jakob disease subtypes. J Biol Chem 2012, 287: 36465–36472.

53 Wadsworth JD, Asante EA, Desbruslais M, Linehan JM, Joiner S, Gowland I, Welch J and Stone L, et al. Human prion protein with valine 129 prevents expression of variant CJD phenotype. Science 2004, 306: 1793–1796.

54 DeMarco ML and Daggett V. From conversion to aggregation: protofibril formation of the prion protein. Proc Natl Acad Sci USA 2004, 101: 2293–2298.

55 Rivillas-Acevedo L, Grande-Aztatzi R, Lomeli I, Garcia JE, Barrios E, Teloxa S and Vela A, et al. Spectroscopic and electronic structure studies of copper(II) binding to His111 in the human prion protein fragment 106-115: evaluating the role of protons and methionine residues. Inorg Chem 2011, 50: 1956–1972.

56 Jones CE, Klewpatinond M, Abdelraheim SR, Brown DR and Viles JH. Probing copper^{2+} binding to the prion protein using diamagnetic nickel^{2+} and 1H NMR: the unstructured N terminus facilitates the coordination of six copper^{2+} ions at physiological concentrations. J Mol Biol 2005, 346: 1393–1407.

57 Klewpatinond M and Viles JH. Fragment length influences affinity for Cu^{2+} and Ni^{2+} binding to His96 or His111 of the prion protein and

58 Hasnain SS, Murphy LM, Strange RW, Grossmann JG, Clarke AR, Jackson GS and Collinge J. XAFS study of the high-affinity copper-binding site of HuPrP(91-231) and its low-resolution structure in solution. J Mol Biol 2001, 311: 467–473.

59 Barducci A, Chelli R, Procacci P, Schettino V, Gervasio FL and Parrinello M. Metadynamics simulation of prion protein: beta-structure stability and the early stages of misfolding. J Am Chem Soc 2006, 128: 2705–2710.

60 Barducci A, Chelli R, Procacci P and Schettino V. Misfolding pathways of the prion protein probed by molecular dynamics simulations. Biophys J 2005, 88: 1334–1343.

61 Alonso DO, DeArmond SJ, Cohen FE and Daggett V. Mapping the early steps in the pH-induced conformational conversion of the prion protein. Proc Natl Acad Sci USA 2001, 98: 2985–2989.

62 Glockshuber R, Hornemann S, Billeter M, Riek R, Wider G and Wuthrich K. Prion protein structural features indicate possible relations to signal peptidases. FEBS Lett 1998, 426: 291–296.

63 Knolmurodov K, Hirano Y and Ebisuzaki T. MD simulations on the influence of disease-related amino acid mutations in the human prion protein. Chem-Bio Inf J 2003, 3: 86–95.

64 De Simone A, Dodson GG, Verma CS, Zagari A and Fraternali F. Prion and water; tight and dynamical hydration sites have a key role in structural stability. Proc Natl Acad Sci USA 2005, 102: 7535–7540.

65 James TL, Liu H, Ulyanov NB, Farr-Jones S, Zhang H, Donne DG and Kaneko K, et al. Solution structure of a 142-residue recombinant prion protein corresponding to the infectious fragment of the scrapie isoform. Proc Natl Acad Sci USA 1997, 94: 10086–10091.

66 Peretz D, Williamson RA, Matsunaga Y, Serban H, Pinilla C, Bastidas RB and Rozenshteyn R, et al. A conformational transition at the N-terminus of the prion protein features in formation of the scrape isoform. J Mol Biol 1997, 273: 614–622.

67 Yuan FF, Biffin S, Brazier MW, Suzrez M, Cappai R, Hill AF and Collins SJ, et al. Detection of prion epitopes on PrPc and PrPsc of transmissible spongiform encephalopathies using specific monoclonal antibodies to PrP. Immunol Cell Biol 2005, 83: 632–637.

68 Sauve S, Buijs D, Gingras G and Aubin Y. Interactions between the conserved hydrophobic region of the prion protein and dodecylphosphocholine micelles. J Biol Chem 2012, 287: 1915–1922.

69 Case DA, Darden TA, Cheatham TE, Simmerling CL, III, Wang J, Duke RE and Luo R, et al. AMBER 11. San Francisco: University of California, 2010.

spectroscopic evidence for a multiple histidine binding only at low pH. Biochem J 2007, 404: 393–402.